03

Heat transfer and critical heat fluxes in short microchannels during boiling of zeotropic mixtures

© A.S. Shamirzaev

Kutateladze Institute of Thermophysics, Siberian Branch, Russian Academy of Sciences, Novosibirsk, Russia
E-mail: alisham@itp.nsc.ru

Received November 3, 2023
Revised November 23, 2023
Accepted November 23, 2023

A study of heat transfer during saturated boiling of zeotropic mixtures of propane–isobutane (R290–R600a) and difluoromethane–tetrafluoroethane (R32–R134a) was carried out in a system of two microchannels 16 mm long (section 2×0.2 mm) at mass fluxes up to 1350 kg/(m$^2 \cdot$ s). It has been established that under conditions of high mass fluxes, the latent heat of vaporization of the mixture does not have a noticeable effect on the value of the critical heat flux, and the critical heat flux is determined by friction in the channel.

Keywords: boiling, binary zeotropic mixtures, critical heat flux, microchannels.

DOI: 10.61011/PJTF.2024.05.57177.19794

The heat transfer of mixed refrigerants is being studied extensively at present with the aim of production of highly efficient and environmentally safe heat transfer systems. Much attention is paid to the feasibility of application of saturated hydrocarbons as replacements for fluorine-containing refrigerants. The optimization of operation of devices relying on different thermodynamic cycles is one of the goals of current research [1,2]. Owing to a large specific area and to the utilization of latent heat of vaporization, boiling in microchannels does not only provide substantial heat removal with a smaller amount of refrigerant, but also maintains a more uniform temperature distribution.

The concentrations of components in liquid and vapor phases in zeotropic mixtures differ. This provides an opportunity to raise the critical vapor fraction by suppressing the growth of dry spots due to delayed evaporation of the „high-boiling" mixture component [3]. At the same time, additional thermal diffusion resistance reduces heat transfer coefficients (HTCs) in phase transitions compared to the results of calculations for an „ideal" mixture. The additional resistance is commonly calculated based on the difference between boiling and condensation temperatures of the mixture (temperature glide). At the same time, the HTCs of certain known mixtures do not degrade at high heat fluxes. The HTC values measured for an R134a–R245fa mixture with a mass concentration of components of 0.9–0.1 boiling in a large volume under high heat fluxes exceed the results of „ideal calculations," and the critical heat flux (CHF) is 35.8 W/cm^2 [4]. Boiling in a heat exchanger with channels with a 2×1 mm cross section, the same mixture at a mass flux of 400 kg/(m$^2 \cdot$ s) provided CHF = 33 W/cm^2 and HTC = 20 kW/(m$^2 \cdot$ K) at a wall temperature of 46°C. The CHF increases at greater subcooling and mass fluxes [1–3,5].

Heat transfer crisis in microchannel heat exchangers is associated primarily with drying out of the surface, and the CHF is expected to increase in short heat exchangers. At present, the majority of studies focused on heat transfer in boiling of zeotropic mixtures are performed in systems with channels with a characteristic size on the order of 1 mm with the aim of optimizing the operation of existing devices. Notably, the Laplace constant

$$l_\sigma^2 = \sigma/\big(g(\rho_l - \rho_v)\big)$$

(ρ_l, ρ_v are the liquid and vapor densities and σ is the surface tension coefficient), which characterizes the scope of influence of capillary forces, is close to that value. The processes of heat transfer of zeotropic mixtures under a dominant influence of capillary forces remain understudied. The aim of the present study is to examine heat transfer in short microchannels under a substantial influence of capillary forces and determine the effect of mass flux on the CHF. A difluoromethane–tetrafluoroethane (R32–R134a) mixture, which has a high coefficient of performance [6], and a hydrocarbon propane–isobutane (R290–R600a) mixture were chosen for examination as examples of environmentally safe zeotropic mixtures.

The experimental section for examination of heat transfer in boiling in short microchannels is a copper assembly with heater cartridges 16 mm in length and two microchannels with a width of 2 mm and a depth of 0.2 mm. A galvanic matte nickel coating 5 μm in thickness was deposited onto the experimental section surface to prevent its oxidation. The entrance and exit chambers of the section have a diameter of 8 mm and a length of 6 mm. In experiments, the temperature and pressure at the section entrance and exit and the temperature gradient in the copper assembly were measured. The experimental setup and the measurement procedure have been discussed in detail earlier in [7]. The diagram of the setup is shown in Fig. 1.

The study was performed at mass fluxes up to 1350 kg/(m$^2 \cdot$ s). A slightly subcooled (by 1–5°C) mixture was supplied to the entrance of the experimental sec-

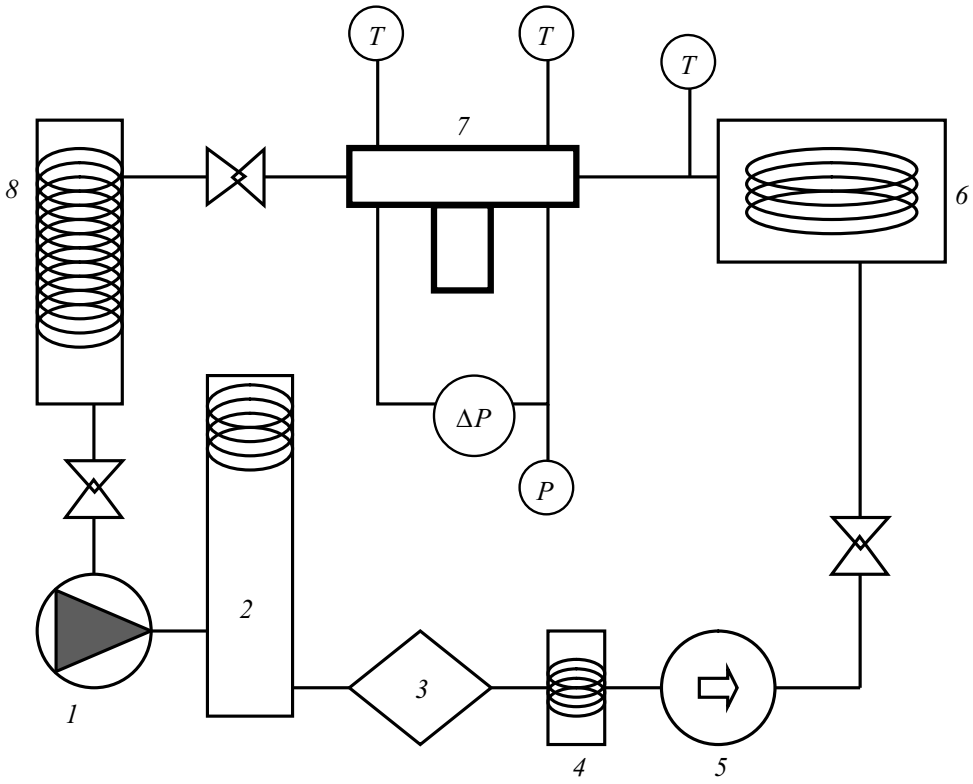

Figure 1. Diagram of the experimental setup. *1* — Dosing pump, *2* — pulsation damper, *3* — filter, *4* — cooler, *5* — mass flow meter, *6* — adjustable thermostat, *7* — experimental section, and *8* — condenser. *T* and *P* denote the points of temperature and pressure measurement, respectively.

Table 1. Properties of mixtures

Mixture	Molar fractions	P/P_{cr}	T/T_{cr}	ρ_l, kg/m^3	ρ_v, kg/m^3	h_{lv}, kJ/kg	k_l, W/(m · K)	σ, 10^{-3} N/m	μ_l, 10^{-3} Pa · s	$\Delta T_{bd}^{\max}$, K
R32−R134a	0.65/0.35 0.54/0.46	0.22	0.82	1086−1100	37−45	226−233	0.124−0.129	7.6−8.5	0.144−0.152	6.7
R290−R600a	0.64/0.36 0.44/0.56	0.17	0.79	500−511	12−17	317−335	0.087−0.091	7.1−8.2	0.112−0.132	7.8

tion. In experiments with R32−R134a, the temperature and pressure of the supplied mixture were $T_0 = 18.0 \pm 0.5°C$ and $P_0 = 11$ bar; the corresponding values in experiments with R290−R600a were $28 \pm 2°C$ and 8 bar. The pressure range was chosen so that the temperatures of phase transitions of mixtures differed approximately by 10°C.

The composition of liquid and vapor phases of a mixed refrigerant changes in the process of boiling, thus altering the thermophysical properties of the mixture. The key properties of the examined mixtures under conditions of the discussed experiment are listed in Table 1 for the actual range of variation of molar fractions in the liquid phase. The studied mixtures have similar values of σ, temperature glide ΔT_{bd}, and liquid viscosity μ_l and thermal conductivity k_l. Mixture R290−R600a has a significantly higher latent heat of vaporization h_{lv} than R32−R134a, but its ρ_l and ρ_v are more than two times lower. It is reasonable to expect that R290−R600a should have greater values of CHF, HTC, and pressure differential than R32−R134a at the same mass flux and heat flux.

Dependences of heat flux q_w on wall temperature T_w are shown in Fig. 2, *a*. At heat fluxes up to 10 W/cm^2, single-phase convection is the dominant heat transfer mechanism. At higher heat fluxes, the heat transfer depends only weakly on the mass flux, and bubble boiling becomes the dominant heat transfer mechanism. An increase in mass flux G leads to an increase in CHF. The values of CHF for mixtures with the same mass flux are close, but, contrary to expectations, the CHF for mixture R32−R134a is somewhat higher than the one for R290−R600a. Bubble boiling is suppressed prior to dryout. This is most noticeable in the dependences of the heat flux on the wall temperature at a mass flux of 550−555 kg/(m^2 · s) for both mixtures. The heat transfer drops first, and only then the transition to dryout occurs

Table 2. Calculation method

Technique of calculation of heat transfer in boiling of binary mixtures [8]	Comment
$\mathrm{HTC} = \left[(F \cdot \mathrm{HTC}_c)^2 + (S_{mix} S \cdot \mathrm{HTC}_b)^2\right]^{0.5}$	Calculation formula
$\mathrm{HTC}_c = 0.023 \mathrm{Re}_l^{0.8} \mathrm{Pr}_l^{0.4} (k_l / D_h)$	Heat transfer in single-phase convection
$\mathrm{HTC}_b = \left[\sum (x_i / \mathrm{HTC}_{b,i})\right]^{-1}$	Heat transfer in boiling of an „ideal“ mixture
$\mathrm{HTC}_{b,i} = 0.55 (P_i / P_{cr,i})^{0.12} M_i^{-0.5} q^{0.67} \left[-\lg (P_i / P_{cr,i})\right]^{-0.55}$	Heat transfer in boiling of component i
$F = \left[1 + X \mathrm{Pr}_l (\rho_l / \rho_v - 1)\right]^{0.35}$	Convection intensification factor
$S = \left(1 + 0.055 F^{0.1} \mathrm{Re}_l^{0.16}\right)^{-1}$	Boiling suppression factor
$S_{mix} = \left(1 + \frac{\Delta T_{db}}{\Delta T_{id}} \lvert y_1 - x_1 \rvert^{-0.29} \left(P \cdot 10^{-5}\right)^{-0.9} \left(1 - 0.87 \exp(-q \cdot 10^{-5}/3)\right)\right)^{-1}$	Factor related to the thermal diffusion resistance (index 1 denotes the low-boiling component)
$\Delta T_{id} = q / \mathrm{HTC}_{id}$, $\mathrm{HTC}_{id} = \left[\sum (x_i / \mathrm{HTC}_i)\right]^{-1}$	
$\mathrm{HTC}_i = \left[\left(F \cdot \mathrm{HTC}_{c,i}\right)^2 + \left(S \cdot \mathrm{HTC}_{b,i}\right)^2\right]^{0.5}$	Heat transfer in flow boiling for each component

Note. Pr_l — Prandtl number, x_i — molar concentration of the ith component in liquid, y_i — molar concentration of the ith component in vapor, M_i — molar mass, X — vapor fraction, ΔT_{db} — temperature glide at the current molar concentration of vapor.

(Fig. 2, *a*). Prior to the onset of dryout, annular flow develops in channels, and crisis is initiated by the emergence of dry spots on the channel walls.

At $G = 1350\,\mathrm{kg/(m^2 \cdot s)}$, the HTC values agree well with the data calculated in accordance with the procedure detailed in [8] (Table 2) at heat fluxes up to $60\,\mathrm{W/cm^2}$ for mixture R290–R600a and up to $120\,\mathrm{W/cm^2}$ for R32–R134a (Fig. 2, *b*). The deviation of measured HTC values from calculated data is indicative of suppression of nucleate boiling. Crisis phenomena in mixture R290–R600a, which has a lower liquid and gas density (and, consequently, a higher flow velocity), are manifested earlier than in mixture R32–R134a. The dependences of HTC on the heat flux for these mixtures differ only slightly.

The authors of [9] have examined heat transfer in boiling of six mixtures in microchannels and proposed a correlation for calculating critical vapor fraction X_{cr} at which dry spots emerge for an azeotropic mixture:

$$X_{cr} = \min\left\{1.21 \mathrm{Re}_{l0}^{-0.13} (\mathrm{Bo} \cdot 10^3)^{-0.16} \mathrm{We}_{l0}^{0.15} \mathrm{Co}^{-0.32} \beta^{0.09}; 0.95\right\}, \quad (1)$$

where $\mathrm{Re}_{l0} = GD_h/\mu$ is the Reynolds number, $\mathrm{Bo} = q_w/(Gh_{lv})$ is the boiling number, $\mathrm{We}_{l0} = (G^2 D_h)/(\rho_l \sigma)$ is the Weber number, D_h is the hydraulic diameter of a channel, and $\beta < 1$ is the ratio of its sides. The attainment of X_{cr} in [9] effectively corresponds to the attainment of CHF. Knowing the composition and the inlet temperature and pressure of a mixture and using the phase equilibrium condition, one may calculate the CHF value. Figure 3, *a* presents a comparison of experimental data on the dependence of CHF on the mass flux with the results of calculations by formula (1). The calculated data agree qualitatively with the experimental ones for R290–R600a, but the calculated CHF value for mixture R32–R134a is significantly lower than the measured CHF. Calculation methods relying on dimensionless complexes do not provide an opportunity to calculate the CHF correctly. Since dryout at high mass and heat fluxes develops in the annular flow regime, the stability of film flow is an important factor specifying the conditions of attainment of CHF. When a single-phase mixture is supplied to the entrance of microchannels, flow regimes change rapidly along the channel length at high heat fluxes. While bubble boiling persists in a certain part of the channel, flow perturbations produced during vapor formation at boiling centers should propagate downstream. As was noted in [10], perturbations affect the wave structure of film, enhancing the amplitude of three-dimensional waves. This is a factor contributing to the intensification of heat transfer. Large-amplitude waves may support nucleation processes that help maintain high heat transfer coefficients. The wave structure of a liquid film surface and the friction stress at the interphase boundary should be related directly; therefore, the pressure differential in a channel and critical heat fluxes should also be related. The results of analysis of experimental data verified

this hypothesis. Figure 3, *b* presents the dependence of CHF on friction stress τ that was determined as $\tau = (\Delta P_{total} - \Delta P_{entr} - \Delta P_{exit})D_h/(4L)$, where L is the channel length, ΔP_{total} is the total measured pressure differential, and ΔP_{entr} and ΔP_{exit} are the entrance and exit pressure losses calculated in accordance with the procedures specified in [11]. Under the conditions of the experiment at $\tau > 8$ kPa, mixtures have similar dependences of CHF on the friction stress. At $\tau < 8$ kPa, the CHF for mixture R290–R600a is higher than the corresponding value for R32–R134a. However, these conditions correspond to heat fluxes below 110 W/cm^2, and the CHF for mixture R32–R134a under such conditions corresponds to near-full evaporation of liquid (Fig. 3, *a*).

Thus, it was found that shortening and miniaturization of channels provide an opportunity to increase considerably the critical heat fluxes during boiling of zeotropic mixtures in microchannels. Critical heat fluxes at the microchannel wall were determined: 147 W/cm^2 for R290–R600a and 153 W/cm^2 for R32–R134a at a mass flux of 1350 kg/(m^2 · s). A relation between the pressure differential in a channel and the critical heat flux value was established. The substitution of R290–R600a with R32–R134a and a 10°C reduction in the phase transition temperature resulted in a corresponding reduction in the wall temperature within almost the entire range of heat fluxes. It should be noted that a mere change in pressure would lead to a reduction in the vapor density of a mixture and, consequently, to an enhancement of friction and earlier manifestation of crisis phenomena. The obtained results indicate that boiling of zeotropic mixtures may well be used for cooling of various types of heat-stressed equipment within a wide temperature range.

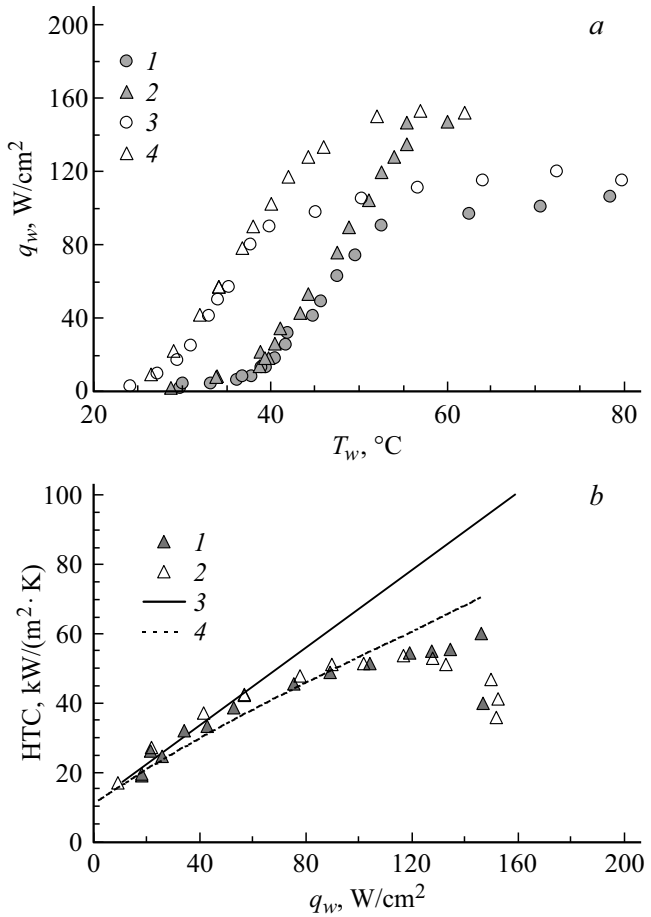

Figure 2. *a* — Dependence of the heat flux on the wall temperature. *1*, *2* — R290–R600a mixture ($G = 555$ and 1350 kg/(m^2 · s), respectively); *3*, *4* — R32–R134a mixture ($G = 550$ and 1350 kg/(m^2 · s), respectively). *b* — Dependence of heat transfer coefficients on the heat flux at $G = 1350$ kg/(m^2 · s) for R290–R600a (*1* — measured values, *3* — data calculated in accordance with [8]) and R32–R134a (*2* — measured values, *4* — data calculated in accordance with [8]).

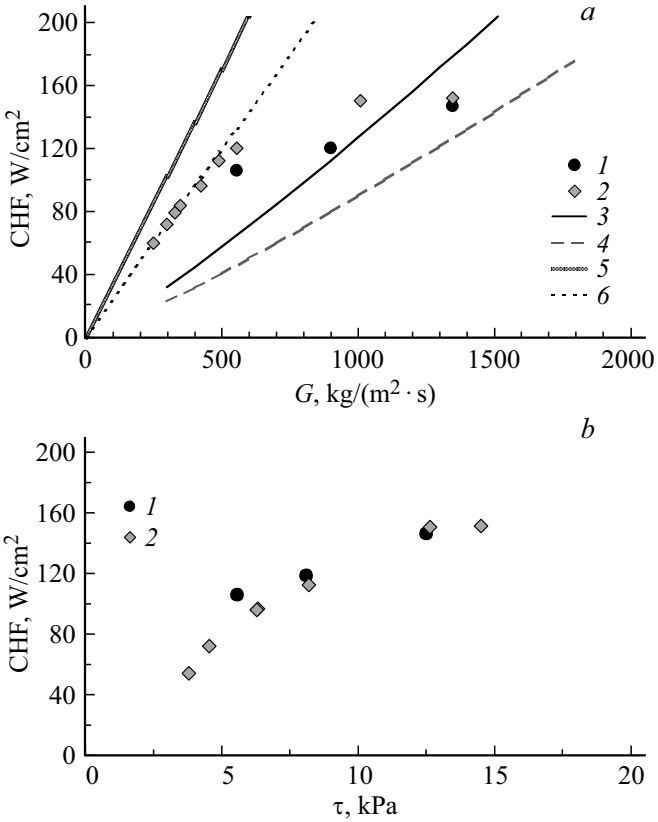

Figure 3. *a* — Dependence of the critical heat flux on the mass flux. Points denote the measured values for mixtures R290–R600a (*1*) and R32–R134a (*2*), while lines correspond to calculations performed in accordance with [9] for R290–R600a (*3*) and R32–R134a (*4*) and full evaporation for R290–R600a (*5*) and R32–R134a (6). *b* — Friction stress in the channel for R290–R600a (*1*) and R32–R134a (*2*).

Funding

This study was carried out at the Kutateladze Institute of Thermophysics of the Siberian Branch of the Russian Academy of Sciences. It was supported by grant No. 22-29-00168 from the Russian Science Foundation (https://rscf.ru/project/22-29-00168/) (experiments with

R32−R134a) and performed under state assignment 121031800215-4 (experiments with R290−R600a).

Conflict of interest

The author declares that he has no conflict of interest.

References

[1] Q. Blondel, N. Tauveron, G. Lhermet, N. Caney, Appl. Therm. Eng., **219**, 119418 (2023). DOI: 10.1016/j.applthermaleng.2022.119418
[2] Z. Ji, M.E. Mondejar, F. Haglind, Appl. Therm. Eng., **150**, 824 (2019). DOI: 10.1016/j.applthermaleng.2019.01.036
[3] C. Dang, L. Jia, Q. Peng, L. Yin, Z. Qi, Int. J. Heat Mass Transfer, **127**, 758 (2018). DOI: 10.1016/j.ijheatmasstransfer.2018.08.083
[4] C. Dang, L. Jia, Q. Peng, Q. Huang, X. Zhang, Int. J. Heat Mass Transfer, **119**, 508 (2018). DOI: 10.1016/j.ijheatmasstransfer.2017.11.143
[5] M.M. Shah, Fluids, **8**, 90 (2023). DOI: 10.3390/fluids8030090
[6] Q. Wang, X. Liu, M. Li, D. Su, C. Dang, J. Peng, B. Hou, L. Dong, Appl. Therm. Eng., **236**, 121724 (2024). DOI: 10.1016/j.applthermaleng.2023.121724
[7] V.V. Kuznetsov, A.S. Shamirzaev, Tech. Phys. Lett., **44**, 938 (2018). DOI: 10.1134/S1063785018100279.
[8] X. Zou, M.Q. Gong, G.F. Chen, Z.H. Sun, Y. Zhang, J.F. Wu, Int. J. Refrig., **33**, 371 (2010). DOI: 10.1016/j.ijrefrig.2009.10.013
[9] D. Jige, M. Nobunaga, T. Nogami, N. Inoue, Appl. Therm. Eng., **229**, 120613 (2023). DOI: 10.1016/j.applthermaleng.2023.120613
[10] E.A. Chinnov, I.A. Sharina, Tech. Phys. Lett., **44**, 969 (2018). DOI: 10.1134/S1063785018110044.
[11] S.G. Kandlikar, S. Garimella, D. Li, S. Colin, M.R. King, *Heat transfer and fluid flow in minichannels and microchannels* (Elsevier, 2006), p. 203.

Translated by D.Safin